Math. Model. Nat. Phenom.
Vol. 11, No. 5, 2016, pp. 33–48
DOI: 10.1051/mmnp/201611503

The Effect of Cell Death on the Stability of a Growing Biofilm

H. A. Wallace, L. Li, F. A. Davidson *

University of Dundee

Abstract. In this paper, we investigate the role of cell death in promoting pattern formation within bacterial biofilms. To do this we utilise an extension of the model proposed by Dockery and Klapper [13], and consider the effects of two distinct death rates. Equations describing the evolution of a moving biofilm interface are derived, and properties of steady state solutions are examined. In particular, a comparison of the planar behaviour of the biofilm interface in the different cases of cell death is investigated. Linear stability analysis is carried out at steady state solutions of the interface, and it is shown that, under certain conditions, instabilities may arise. Analysis determines that, while the emergence of patterns is a possibility in 'deep' biofilms, it is unlikely that pattern formation will arise in 'shallow' biofilms.

Keywords and phrases: biofilm, expansion, cell-death, mathematical modelling, free boundary

Mathematics Subject Classification: 92C15, 35R37

1. Introduction

It is widely believed that almost all bacterial biomass is located within complex, close-knit communities called biofilms, which are found at solid-liquid, liquid-air or solid-air interfaces [20]. They can comprise a single microbial species or more typically multiple species depending on environmental parameters [12,27]. Biofilms that are composed of multiple species can be found in most natural environments, while biofilms that are formed by single species are much less common and tend to exist in specific infection sites, for example on the surface of medical implants [7, 27]. Most biofilms exhibit heterogeneity to some extent [6,12,14,23] i.e. rather than consisting of a continuous homogeneous layer, biofilms contain microcolonies of bacterial cells separated from other microcolonies by interstitial voids (water channels).

A defining characteristic of the biofilm is that the bacteria are encased within a self-produced extracellular matrix [4,21,25], composed of a mixture of components including extracellular polymeric substance (EPS). The production of EPS, accounting for 50% to 90% of the total biomass of the biofilm [14], involves a significant investment of energy and thus it is assumed that this sticky matrix must be beneficial for growth by offering environmental protection [25]. In particular, EPS is thought to contribute to the increased antimicrobial resistance that is displayed in wildtype biofilms in comparison to *eps* mutants [11,21].

*Corresponding author. E-mail: f.a.davidson@dundee.ac.uk

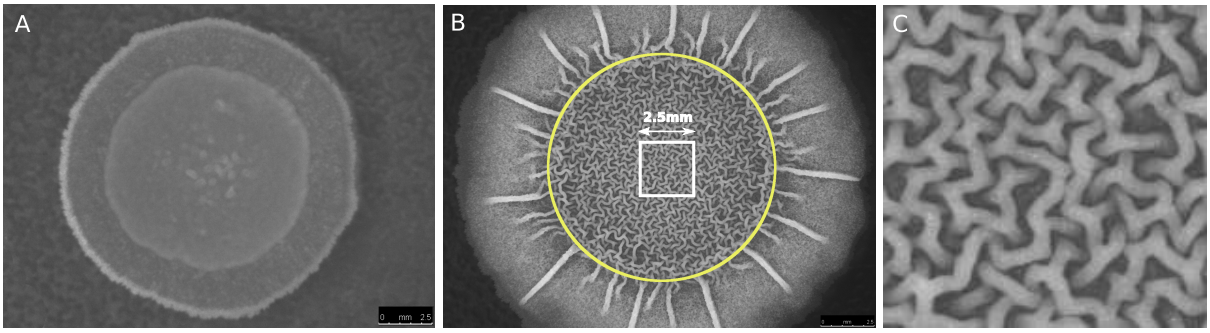

FIGURE 1. Morphology of wildtype *Bacillus subtilis* biofilm grown at 30°C on 1.5% agar substrate. Figure A: Early biofilm (18 hours into growth) shows homogeneity. Figure B: Mature biofilm (48 hours into growth) shows complex heterogeneous pattern within the coffee-ring region (yellow outline). A close-up of the highlighted white square is shown in Figure C, where the intricate rope-like wrinkle structure within the coffee-ring can be observed. Photographs by L. Li (unpublished).

Many different mathematical approaches have been proposed as a way of modelling the development of bacterial biofilms. These techniques include cellular automata models [22,32], partial differential equation models [1,17,26], and in particular moving boundary problems implementing a fluid dynamics approach [2,10,13,19]. Free or moving boundary (or Stefan) problems, characterised by a space and time dependent moving boundary that must be tracked throughout development as part of the solution [8], present complex mathematical challenges. Nonlinearity arising through the coupling of material and interface dynamics, and the inclusion of multiple time and length scales, contribute to the difficulties associated with these problems [24]. As a result of these complications, numerical rather than analytical techniques are generally used to determine behaviour, except in some special simplified cases [16].

Dockery and Klapper [13] presented a simple moving boundary model of a single substrate limited biofilm growing into a static aqueous environment. They deduced that the biofilm interface is linearly unstable to fingering instabilities under certain conditions. In this paper we build on the model derived in [13] to consider the case of biofilm growth on a surface in which the growth limiting substrate is assumed to be oxygen in the air above. The growth surface represents agar in a typical laboratory experiment where penetration into the agar is minimal and nutrients within the medium are not limiting for growth (initially in any case). Under these conditions complex biofilm morphologies can be produced, particularly in mature biofilms, which are often not of uniform depth and indeed can form elaborate, heterogeneous large scale structures [1,3,5,33] (see Figure 1). We extend the model formulated in [13] by introducing a new cell death term to represent the findings of Asally et al. [1], which state that cell death at the base of biofilms acts as a precursor to wrinkling, specifically within the central region of the biofilm (i.e. the 'coffee-ring' region, which can be seen in Figure 1B). We examine the effect that cell death has on the growth of the biofilm and the heterogeneity and patterning displayed.

2. Model set up

The model set-up used in this paper follows much the same formulation as in [13]. However, rather than considering a biofilm growing into an aqueous environment, we investigate a non-submerged biofilm growing on an agar substrate into the air above. For convenience, an overview of the model set-up is described here (full details can be found in [13]), and a schematic of the set-up is shown in Figure 2.

The domain of interest $D \subset \mathbb{R}^3$ is an unbounded slab separated by a surface $z = h(\mathbf{x}, t)$ (where $\mathbf{x} = (x, y)$), into two regions: (i) the biofilm in $0 < z < h(\mathbf{x}, t)$, and (ii) the air above in $z > h(\mathbf{x}, t)$. Oxygen is assumed here to be the growth limiting substrate and is denoted by $s = s(\mathbf{x}, z, t)$.

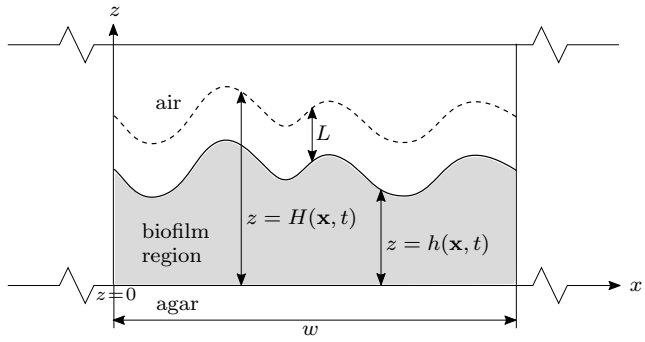

FIGURE 2. Schematic of model set-up. The biofilm grows on an agar substrate and expands vertically into the air above. The x and z-directions are labelled (y points into the page), as is the characteristic length scale w. The biofilm-agar interface is positioned at $z = 0$.

In the lower region, the biofilm itself is modelled as a viscous, homogeneous, incompressible fluid with constant density, rescaled here to unity. The velocity, $\mathbf{u}$, of this fluid is related to the pressure, $p(\mathbf{x}, z, t)$ (or more specifically the pressure gradient $\nabla p(\mathbf{x}, z, t)$), within the biofilm via a standard relationship, namely,

$$\mathbf{u} = -\lambda \nabla p, \tag{2.1}$$

where λ is a positive constant (note that this relationship is often referred to as Darcy's Law in certain specific contexts). Cell growth and division generates a source of mass within the biofilm which is taken into account within the conservation of mass equation,

$$\nabla \cdot \mathbf{u} = g, \tag{2.2}$$

where $g = g(s)$ is some growth function that models the net production of bacteria per unit volume per unit time. Combining (2.2) with (2.1) yields a relationship between growth and resultant pressure such that

$$-\lambda \nabla^2 p = g(s). \tag{2.3}$$

Cell maintenance and growth require substrate (in this case oxygen). Substrate consumption is modelled by an expression of the form $f(s)$ and thus substrate concentration within the biofilm region is governed by the equation

$$s_t = D_2 \nabla^2 s - f(s), \tag{2.4}$$

where $D_2 > 0$ is a standard Fickian diffusion coefficient. Clearly, the growth function, g, and substrate utilisation, f, are related as will be discussed later.

Substrate concentration in the upper region, $h(\mathbf{x}, t) < z < H(\mathbf{x}, t)$, is again assumed to diffuse in a standard Fickian manner and is thus governed by the equation

$$s_t = D_1 \nabla^2 s, \tag{2.5}$$

where D_1 is a positive constant. It is reasonably assumed that substrate concentration far above the biofilm interface is unaffected by biofilm growth. Thus substrate is assumed to be a constant above a height denoted by $H(\mathbf{x}, t)$=$h(\mathbf{x}, t) + L$, where L is a constant. Finally, in the upper region, we set pressure $p \equiv 0$. In fact, we define the interface separating the upper and biofilm regions by $p = 0$.

To complete the model, boundary conditions are imposed as follows: The biofilm-agar interface ($z = 0$) is assumed impermeable to the biofilm, and therefore the z-component of velocity is zero here. Consistent with this condition, $p_z(\mathbf{x}, 0, t) = 0$. Similarly, the flux of substrate across the boundary is set to be zero at

$z = 0$. At the biofilm surface $z = h(\mathbf{x}, t)$, the pressure is assumed to be zero. Indeed this defines the location of the tracked interface via the interface equation given below. Moreover, the substrate concentration is assumed continuous at the interface $z = h(\mathbf{x}, t)$, and a flux continuity condition is imposed as detailed below. Finally, the substrate concentration is set constant for $z > H(\mathbf{x}, t)$. In summary, the applied boundary conditions are as follows:

$$p|_{z=h} = 0, \quad p_z|_{z=0} = 0; \tag{2.6a}$$

$$s|_{z=H} = s_\infty, \quad s_z|_{z=0} = 0; \tag{2.6b}$$

$$s|_{z=h^+} = s|_{z=h^-}; \tag{2.6c}$$

$$\mathbf{n} \cdot D_1 \nabla s|_{z=h^+} = \mathbf{n} \cdot D_2 \nabla s|_{z=h^-}, \tag{2.6d}$$

along with the interface equation

$$\frac{\partial h}{\partial t} = -\mathbf{n} \cdot \lambda \nabla p|_{z=h^-}, \tag{2.7}$$

where h^+ and h^- denote the biofilm interface approached from above and below respectively, $\mathbf{n}$ denotes the (upward pointing) normal to the interface $z = h$ and s_∞ is a positive constant representing the bulk substrate concentration.

3. Non-dimensionalisation

Some scaling factors are introduced to simplify the model. Wildtype biofilms of *B. subtilis* grown on agar, despite generally having much greater length than height, appear to develop spatial features with a characteristic length of pattern, denoted w, which are repeated throughout the domain. Experimental observations show that both the characteristic length of patterns and biofilm height are of the same order of approximately $10^2 \mu$m (see for example [34, 37]). Hence, for computational purposes, a domain of fixed height, $\bar{H}$, and width, w, can be employed on which periodic boundary conditions in the x and y-directions can be imposed for the pressure and substrate variables. A time scale, T, associated with biofilm growth can also be introduced. By setting

$$\bar{\mathbf{x}} = \frac{\mathbf{x}}{w}, \bar{z} = \frac{z}{w}, \bar{h} = \frac{h}{w}, \bar{H} = \frac{H}{w}, \bar{L} = \frac{L}{w}, \bar{t} = \frac{t}{T}, S = \frac{s}{s_\infty},$$

$$\bar{f}(s) = \frac{f(s)}{f(s_\infty)}, \bar{g}(s) = g(s)T, P = \frac{\lambda T}{w^2} p,$$

the non-dimensional system can be obtained after dropping bars for simplicity:

$$\epsilon_1 S_t - \nabla^2 S = 0, \qquad h(\mathbf{x}, t) < z < H(\mathbf{x}, t) \tag{3.1}$$

$$\begin{cases} \epsilon_2 S_t - \nabla^2 S = -G f(S); \\ \nabla^2 P = -g(S); \end{cases} \quad 0 < z < h(\mathbf{x}, t) \tag{3.2}$$

with the evolution equation

$$h_t = -\mathbf{n} \cdot \nabla P|_{z=h^-}, \tag{3.3}$$

where $G = \frac{w^2}{s_\infty D_2} f(s_\infty)$, $\epsilon_i = \frac{w^2}{D_i T}$ and we have redefined $\bar{g}(S s_\infty) = \bar{g}(S)$ and $\bar{f}(S s_\infty) = \bar{f}(S)$ by absorbing the constant into the functional definition. Note the (periodically repeating) domain is rescaled such that $(x, y) \in (0, 1) \times (0, 1)$.

Substituting the desired forms of non-dimensional variables into the boundary conditions (2.6) yields the corresponding dimensionless boundary conditions:

$$P|_{z=h} = 0, \quad P_z|_{z=0} = 0; \tag{3.4a}$$

$$S|_{z=H} = 1, \quad S_z|_{z=0} = 0; \tag{3.4b}$$

$$S|_{z=h^+} = S|_{z=h^-}; \tag{3.4c}$$

$$\mathbf{n} \cdot K \nabla S|_{z=h^+} = \mathbf{n} \cdot \nabla S|_{z=h^-}, \tag{3.4d}$$

where $K = D_1/D_2$. As oxygen diffuses more readily through air than the porous medium of the biofilm [9, 30], it can be reasonably assumed that $D_2 < D_1$. Hence, throughout this paper, $K > 1$. It is also assumed that ϵ_1 and ϵ_2 are small up to observable biofilm length scales ω [13], thus $\epsilon_i \ll 1$. As noted in [13], the parameter G, referred to as the *growth number*, has a particular meaning: $G = w^2/l_s^2$ where $l_s = \sqrt{D_2 s_\infty / f(s_\infty)}$ measures the *penetration depth* of substrate into the biofilm i.e. a depth scale over which the diffusible substrate can penetrate before it is consumed. The region $h - l_s < z < h$ is referred to as the active layer of the biofilm, therefore the quantity $1/\sqrt{G}$ is a measure of the active layer depth which can alternatively be thought of as a measure of the efficiency of substrate utilisation.

Finally, the functional forms for f and g must be set. Following [13] we take the simplest, reasonable form for f, namely $f(S) = S$, and use this throughout the paper as a viable approximation to more complete descriptions of appetite-limited substrate utilisation in non-saturated conditions. It is well known that bacterial death occurs in the biofilm [28, 35, 36] and of particular relevance here is recent work that has highlighted the role that cell death plays in mediating heterogeneous growth [1]. Asally et al. [1] highlighted the role of cell death in generating pattern formation in bacterial biofilms grown in laboratory conditions represented by the model set-up considered here. In particular, in [1], it was shown that cell death occurred at the base of *Bacillus subtilis* biofilms (at the biofilm-agar interface). Specifically, it was hypothesised that the resulting cell death pattern within the central coffee-ring region (highlighted in Figure 1B), acts as a pre-pattern for the striking growth patterns of the type illustrated in Figure 1C. To model this phenomena, it is necessary to introduce a death term into the bacterial growth function g i.e. (in non-dimensional form) $g(S) = f(S) - d(S)$ where $d = d(S)$ represents the death of cells, which can be thought of as being associated with cell removal or shrinkage. In [13], most of the analysis considers the case $d \equiv 0$. In this paper we investigate the role of cell death in more detail. In particular we examine two cases: cell death at a constant rate (discussed briefly in [13]) and substrate dependent cell death, motivated by [1]. We therefore consider both $d(S) := \mu$ and $d(S) := \mu(1 - S)$ in turn. The former is the standard constant death term. The latter is a simple model for the phenomenon discussed in [1], where death rate increases with decreasing substrate concentration (corresponding to increasing distance below the biofilm-air interface) and approaches the constant death rate μ below the active layer region. Thus $g(S) = S - \mu$ and $g(S) = (1 + \mu)S - \mu$, respectively. In both cases we present an analysis of the effects of cell death on the development of the biofilm and pattern formation.

In conclusion, on setting $\epsilon_1 = \epsilon_2 = 0$ (a standard analytical approach in the solution of moving boundary problems) and employing the growth and utilisation functions detailed above yields a quasi-static description of equations (3.1) and (3.2):

$$\nabla^2 S = 0; \qquad h(\mathbf{x}, t) < z < H(\mathbf{x}, t) := h(\mathbf{x}, t) + L, \tag{3.5}$$

$$\begin{cases} \nabla^2 S = GS; \\ \nabla^2 P = -D_\mu S + \mu; \end{cases} \quad 0 < z < h(\mathbf{x}, t) \tag{3.6}$$

that is to be solved in conjunction with the interface evolution equation (3.3) and boundary conditions (3.4). Here

$$D_\mu = \begin{cases} 1, & d(S) := \mu, \\ 1 + \mu, & d(S) := \mu(1 - S), \end{cases} \tag{3.7}$$

where μ is a positive constant. As an aside we note that setting $D_\mu = 1$ and $\mu = 0$ in equation (3.6) recovers the case where no cell death occurs ($d \equiv 0$), which is the main focus in [13].

The paper is organised as follows. Planar solutions to equations (3.5)-(3.6) are found and differences between behaviour at the steady states in the different cases of cell death are noted. Following this, the corresponding non-planar solutions are derived and the possibility of pattern formation occurring at steady states is investigated in both 'shallow' and 'deep' biofilms (as explained later).

4. Planar solutions

First, we consider the effects of cell death on planar solutions. From (3.5)-(3.6), planar solutions $S_0(z,t), P_0(z,t)$ and $h_0(t)$ must satisfy

$$S_{0,zz} = 0 \qquad h_0(t) < z < H_0 := h_0(t) + L. \tag{4.1}$$

$$\begin{cases} S_{0,zz} = GS_0; \\ P_{0,zz} = -D_\mu S_0 + \mu; \end{cases} \qquad 0 < z < h_0(t) \tag{4.2}$$

where the boundary conditions for planar solutions are

$$P_0\,|_{z=h_0} = 0\,, \quad P_{0,z}\,|_{z=0} = 0; \tag{4.3a}$$
$$S_0\,|_{z=H_0} = 1, \quad S_{0,z}\,|_{z=0} = 0; \tag{4.3b}$$
$$S_0|_{z=h_0^+} = S_0|_{z=h_0^-}; \tag{4.3c}$$
$$KS_{0,z}|_{z=h_0^+} = S_{0,z}|_{z=h_0^-}; \tag{4.3d}$$

and the interface evolution equation is

$$h_0'(t) = -P_{0,z}|_{z=h_0}. \tag{4.4}$$

Solving (4.1)-(4.3), it follows that the planar solution for the substrate is

$$S_0(z,t) = \begin{cases} 1 - \bar{S}K^{-1}\sqrt{G}\tanh(\sqrt{G}h_0)(H_0 - z), & h_0(t) < z < H_0; \\ \\ \bar{S}\,\dfrac{\cosh(\sqrt{G}z)}{\cosh(\sqrt{G}h_0)}, & 0 < z < h_0; \end{cases} \tag{4.5}$$

where

$$\bar{S} = \left[1 + LK^{-1}\sqrt{G}\tanh(\sqrt{G}h_0)\right]^{-1}$$

is the value of the substrate at the interface $z = h_0$. Substituting the second expression in (4.5) into the second expression of (4.2), integrating twice and implementing the boundary conditions yields

$$P_0(z,t) = \frac{D_\mu \bar{S}}{G}\left[1 - \frac{\cosh(\sqrt{G}z)}{\cosh(\sqrt{G}h_0)}\right] + \frac{\mu}{2}(z^2 - h_0^2). \tag{4.6}$$

Finally, substitution of (4.6) into the interface evolution equation (4.4) yields

$$h_0'(t) = \frac{D_\mu \bar{S}}{\sqrt{G}}\tanh(\sqrt{G}h_0) - \mu h_0. \tag{4.7}$$

We now examine the effects of cell death on the planar development of the biofilm by focussing on the biofilm-substratum interface h_0 and referring to equation (4.7). A closed form solution for equation (4.7) cannot be obtained, however it is informative to consider the qualitative structure of the solution in each case of cell death. We are only interested in non-negative solutions and it follows directly from standard arguments that solutions of (4.7) with non-negative initial data remain non-negative.

To distinguish between solutions h_0 in the different cases of cell death, the notation h_{0a}, h_{0c} and h_{0s} is used to denote planar solutions in the absence of death (where $D_\mu = 1$ and $\mu = 0$), with constant death (where $D_\mu = 1$) and with substrate dependent death (where $D_\mu = 1 + \mu$), respectively. Immediately, it can be seen that for any given h_0,

$$h_{0a}' > h_{0s}' > h_{0c}', \tag{4.8}$$

representing the fact that biofilm growth at a specific planar height will be fastest when no cell death is present, as one might anticipate. Moreover, for each fixed value of μ, growth at h_0 will also be faster in the case of substrate dependent death compared to constant cell death. Further qualitative details can be found by examining the different death cases in turn.

Firstly, in the case of no cell death, it is clear from (4.7) that for any non-negative h_0, $h'_{0a} > 0$ and

$$\lim_{h_{0a}\to\infty} \bar{S} = \frac{1}{1 + K^{-1}L\sqrt{G}} \implies \lim_{h_{0a}\to\infty} h'_{0a} = \frac{1}{\sqrt{G} + K^{-1}LG}.$$

Thus, given any non-negative initial biofilm height $h_{0a}(0)$, the biofilm is predicted to increase in height (thickness) without bound. Moreover, the growth rate reaches a terminal velocity inversely proportional to the growth number, G, and the length scale, L, of the far-field substrate concentration, and directly proportional to K, a measure of the relative density of the biofilm. This relationship has very natural consequences in that it predicts efficient growth or a closer far-field substrate will induce faster growth, whilst a biofilm more impervious to substrate (smaller K) will grow more slowly.

In the case of positive death rates, $\mu > 0$, it is straightforward to verify from equation (4.7) that

$$\begin{aligned} h'_0(t) &\leq \frac{D_\mu \tanh(\sqrt{G}\, h_0)}{\sqrt{G}} - \mu h_0 \\ &\leq \frac{D_\mu}{\sqrt{G}} \sqrt{G}\, h_0 - \mu h_0 \\ &= (D_\mu - \mu)\, h_0, \end{aligned} \tag{4.9}$$

and hence a sufficient condition for monotonic die-back of the biofilm is $D_\mu < \mu$. Hence, in the case of constant cell death, complete die-back will occur for $\mu > 1$. In the case of substrate dependent cell death, condition (4.9) simplifies to $h'_{0s}(t) \leq h_{0s}$, and therefore (4.9) fails to define any necessary or sufficient conditions to ensure the die-back of a biofilm in the presence of substrate dependent death. Rather, (4.9) simply states that growth in this case can be no faster than exponential.

Considering the interface equation (4.7) in isolation and following standard arguments, it is clear that at least one real steady state, the trivial steady state, exists in both the absence and presence of cell death. While the trivial steady state $h_0^* = 0$ is the singular fixed point in the absence of death and the presence of constant cell death with $\mu > 1$, a second steady state $h_0^* = h_0^*(\mu)$ given implicitly by

$$h_0^*(\mu) = \frac{D_\mu\, \bar{S}^*}{\mu\, \sqrt{G}} \tanh\left(\sqrt{G} h_0^*\right), \tag{4.10}$$

where * denotes evaluation at this steady state, exists in the case of constant cell death where $\mu < 1$ and all cases of substrate dependent death. An examination of extreme parameter cases contributes to a better understanding of steady state behaviour for $\mu > 0$. It is clear that as $\mu \to 0$, $h_0^* \to \infty$. It can also be seen that

$$\begin{aligned} \lim_{\mu\to 0} h'_{0c}(t) = \lim_{\mu\to 0} h'_{0s}(t) =& \frac{\tanh(\sqrt{G}h_0)}{\sqrt{G}\left(1 + LK^{-1}\sqrt{G}\tanh(\sqrt{G}h_0)\right)} \\ =& h'_{0a}(t), \end{aligned} \tag{4.11}$$

therefore as $\mu \to 0$, biofilm growth in the presence of death is expected to follow the same evolutionary behaviour as that in the absence of death, with the biofilm growing without bound. On the other hand, if $\mu \to \infty$, then $h'_{0c} < 0$ and $h^*_{0c} = 0$, while

$$h^*_{0s} \to \frac{\tanh(\sqrt{G}h^*_{0s})}{\sqrt{G}\left(1 + LK^{-1}\sqrt{G}\tanh(\sqrt{G}h^*_{0s})\right)}. \tag{4.12}$$

Moreover, it can be shown by rearrangement of equation (4.10) and implementation of the chain, product and quotient rules, that both $\partial h_{0c}^*/\partial\mu < 0$ and $\partial h_{0s}^*/\partial\mu < 0$. Hence, as may be expected, an increase in cell death results in thinner biofilms overall, regardless of whether death is constant or substrate dependent. Similarly, $\partial h_{0c}^*/\partial G < 0$ and $\partial h_{0s}^*/\partial G < 0$, and thus decreasing substrate penetration depth l_s, where $l_s = 1/\sqrt{G}$, has the effect of decreasing steady state biofilm height.

Standard ODE arguments applied to the interface equation (4.7) in isolation suggest that the singular trivial steady state $h_0^* = 0$ will be unstable in the absence of death, and stable in the presence of constant death where $\mu > 1$. In the case of constant cell death with $\mu < 1$ and all cases of substrate dependent cell death, similar arguments infer that the trivial steady state will be unstable, while the second non-trivial steady state $h_0^*(\mu)$ will be stable to linear perturbations. As a result, it is predicted that in contrast to constant cell death, complete biofilm die-back will never occur in the case of substrate dependent cell death; even for large μ, the biofilm height will reach a positive, steady state value.

In conclusion, a planar analysis of the model predicts that in the absence of cell death, a biofilm with planar surface limited only by substrate diffusion increases in thickness without bound with a terminal velocity determined by the value of the growth parameters. In the case of constant cell death, the model predicts that for sufficiently small death rates ($\mu < 1$) planar height will tend to a steady state with value $h_{0c}^* = h_{0c}^*(\mu)$. For constant cell death at super-threshold levels ($\mu > 1$), biofilm collapse is induced. In the case of a substrate-dependent death rate, the model predicts that the planar height will always tend to a positive steady state with value $h_{0s}^* = h_{0s}^*(\mu)$, regardless of the value of μ. In the following section, we discuss stability of the interface to non-planar perturbations and the role of cell death in this process.

5. Non-planar growth

5.1. General formulation

Next, in order to investigate the stability of the planar solutions to non-planar perturbations, we follow a similar method as described in [13] and consider solutions of (3.3)- (3.6) of the form

$$\begin{aligned} S(\mathbf{x},z,t) &= S_0(z,t) + S_1(z,t)\exp(i\mathbf{k}\cdot\mathbf{x}),\\ P(\mathbf{x},z,t) &= P_0(z,t) + P_1(z,t)\exp(i\mathbf{k}\cdot\mathbf{x}),\\ h(\mathbf{x},t) &= h_0(t) + h_1(t)\exp(i\mathbf{k}\cdot\mathbf{x}), \end{aligned} \tag{5.1}$$

where S_0, P_0 and h_0 are as defined in Section 4, $|S_1| \ll 1, |S_{1,z}| \ll 1, |P_1| \ll 1, |P_{1,z}| \ll 1, |h_1| \ll 1, |h_1'(t)| \ll 1$ and where $\mathbf{k}$ is the 2-dimensional wave number $\mathbf{k} = (k_1, k_2)$ with $|\mathbf{k}| = k$. As in [13], we set $H(\mathbf{x},t) = h_0(t) + L$ for simplicity. On substitution into (3.3)-(3.6), and after following standard arguments, it can be shown that the perturbations $S_1(z,t), P_1(z,t)$ must satisfy

$$S_{1,zz} - k^2 S_1 = 0; \qquad h_0(\mathbf{x},t) < z < H_0(t) \tag{5.2}$$

$$\begin{cases} S_{1,zz} - (k^2+G)S_1 = 0; \\ P_{1,zz} - k^2 P_1 = -D_\mu S_1; \end{cases} \quad 0 < z < h_0(\mathbf{x},t) \tag{5.3}$$

and the interface perturbation $h_1(t)$ satisfies

$$h_1' = -h_1 P_{0,zz}|_{h_0} - P_{1,z}|_{h_0}. \tag{5.4}$$

[This last equation follows from substitution into (3.3) and on using the second equation in (4.2)]. The corresponding boundary conditions for the small perturbations S_1, P_1, h_1 are

$$h_1 P_{0,z}|_{h_0} + P_1|_{h_0} = 0, \quad P_{1,z}|_0 = 0; \tag{5.5a}$$

$$S_1|_{h_0+L} = 0, \quad S_{1,z}|_0 = 0; \tag{5.5b}$$

$$h_1 S_{0,z}|_{h_0^+} + S_1|_{h_0^+} = h_1 S_{0,z}|_{h_0^-} + S_1|_{h_0^-}; \tag{5.5c}$$

$$K\left(h_1 S_{0,zz}|_{h_0^+} + S_{1,z}|_{h_0^+}\right) = h_1 S_{0,zz}|_{h_0^-} + S_{1,z}|_{h_0^-}. \tag{5.5d}$$

[Note that all of the above expressions neglect higher order terms]. Solving for $S_1(z,t)$ in (5.2) and (5.3) and using the boundary conditions (5.5b)-(5.5d) yields:

$$S_1(z,t) = \begin{cases} A_1 \bar{S} h_1 \sqrt{G} \dfrac{\sinh[k(H_0 - z)]}{\cosh[k(H_0 - h_0)]}, & h_0(\mathbf{x},t) < z < H_0(t), \\ B_1 \bar{S} h_1 \sqrt{G} \dfrac{\cosh[\sqrt{k^2+G}z]}{\cosh[\sqrt{k^2+G}h_0]}, & 0 < z < h_0(\mathbf{x},t), \end{cases} \tag{5.6}$$

where $A_1 = A_1(t)$ and $B_1 = B_1(t)$ are constants (w.r.t. z) of integration, that after some algebra can be expressed as

$$\begin{aligned} A_1 =& \frac{(K-1)\sqrt{k^2+G}\,\tanh(\sqrt{G}h_0)\,\tanh(\sqrt{k^2+G}h_0) - \sqrt{G}K}{K\left(\sqrt{k^2+G}\,\tanh(kL)\,\tanh(\sqrt{k^2+G}h_0) + Kk\right)}, \\ B_1 =& -\left(\frac{k(K-1)\tanh(\sqrt{G}h_0) + \sqrt{G}\tanh(kL)}{\sqrt{k^2+G}\,\tanh(kL)\,\tanh(\sqrt{k^2+G}h_0) + Kk}\right). \end{aligned} \tag{5.7}$$

Using (5.6), the second equation in (5.3) yields

$$P_1(z,t) = h_1\left[E_1 e^{kz} + F_1 e^{-kz} - \frac{D_\mu B_1 \bar{S}}{\sqrt{G}} \frac{\cosh(\sqrt{k^2+G}z)}{\cosh(\sqrt{k^2+G}h_0)}\right]. \tag{5.8}$$

Applying the boundary condition (5.5a) and substituting the expression for P_0 given in (4.6) results in $E_1 = F_1$ where

$$E_1 = \frac{1}{2\cosh(kh_0)}\left[\frac{D_\mu \bar{S}}{\sqrt{G}}(B_1 + \tanh(\sqrt{G}h_0)) - \mu h_0\right]. \tag{5.9}$$

Finally, an expression for the first order correction to the interface evolution equation is obtained. On substitution of the expression for $S_0(z,t)$ for $0 < z < h(x,t)$ given in (4.5) into (5.4) and using (5.8), it follows that

$$\begin{aligned} h_1'(t) =& h_1\left[(kh_0\tanh(kh_0) - 1)\mu + D_\mu \bar{S}\left(1 - \frac{k\tanh(kh_0)}{\sqrt{G}}B_1\right) - \right. \\ & \left. D_\mu \bar{S}\left(\frac{k\tanh(kh_0)\tanh(\sqrt{G}h_0)}{\sqrt{G}} - \frac{\sqrt{k^2+G}}{\sqrt{G}}\tanh(\sqrt{k^2+G}h_0)B_1\right)\right], \end{aligned} \tag{5.10}$$

where $B_1 < 0$, and is given in (5.7). It is noted that (5.10) is of the form $h_1'(t) = \omega(k,t)h_1(t)$, where $\omega(k,t)$ is the *dispersive coefficient* of system (3.5)-(3.6) about the planar solutions (4.5)-(4.7). It is clear that the sign of $\omega(k,t)$ may vary depending on the choice of the wave number k and other parameter values. Therefore, the evolving planar solution of system (3.5)-(3.6) is potentially unstable to non-planar perturbations with certain wave numbers.

Notice also that the above linearisation is around a general $h_0 = h_0(t)$, and is therefore valid for all values of h_0. Linearisation around the uniform steady state h_0^*, such that $P_0(z,t) = P_0(z)$ and $S_0(z,t) = S_0(z)$, results in the same system and solutions as defined in equations (5.6)-(5.10) (where h_0 is replaced by h_0^*) due to the fact that the quasi-static description of equations (equations (3.5)-(3.6)) is considered. On substitution of the steady state expression (4.10) into equation (5.10), a specific expression for the evolution of $h_1(t)$ at $h_0 = h_0^*$ in the presence of cell death is found as $h_1^{*'}(t) = h_1(t)\omega^*$, where

$$\omega^* = \mu\left[\frac{h_0^*}{\tanh(\sqrt{G}h_0^*)}\left(\sqrt{G} - k\tanh(kh_0^*)B_1^* + \sqrt{k^2+G}\tanh(\sqrt{k^2+G}h_0^*)B_1^*\right) - 1\right], \tag{5.11}$$

and the superscript * denotes evaluation at the non-trivial steady state h_{0c}^* or h_{0s}^*. Expression (5.11) is the same for both constant and substrate dependent cell death, though recall that the steady state $h_0^* > 0$ only exists for constant cell death if $\mu < 1$, and $h_{0c}^* < h_{0s}^*$ for any fixed value of μ.

5.2. Relevant perturbations and values of k

We note that the above expressions $A_1(t)$ and $B_1(t)$ and thus the non-planar solutions $S_1(z,t)$, $P_1(z,t)$ and $h_1'(t)$ in section 5.1 are undefined at $k=0$. However, non-planar solutions in this special case can be found by substitution of $k=0$ into the equations (5.2)-(5.3) and perturbations (5.1) and solving as above. Comparing the solutions with $k=0$ and $k>0$, it can be shown that

$$\begin{aligned} S_1(k=0,z,t) &= \lim_{k\to 0} S_1(z,t), \\ P_1(k=0,z,t) &= \lim_{k\to 0} P_1(z,t), \\ h_1'(k=0,t) &= \lim_{k\to 0} h_1'(t). \end{aligned} \tag{5.12}$$

Also, at the steady state h_0^*,

$$\omega^*(k=0,t) = \mu\left[\sqrt{G}h_0^*\left(\frac{1}{\tanh(\sqrt{G}h_0^*)} + \hat{B_1^*}\right) - 1\right] = \lim_{k\to 0}\omega^*(k,t), \tag{5.13}$$

where

$$\hat{B_1^*} = -\left(\frac{(K-1)\tanh(\sqrt{G}h_0^*) + \sqrt{G}L}{\sqrt{G}\,L\,\tanh(\sqrt{G}h_0^*) + K}\right) = \lim_{k\to 0} B_1^*. \tag{5.14}$$

It is therefore clear that all solutions can be evaluated at, and are continuous at, $k=0$. We use this limiting case later.

Recall that we are interested in periodic solutions. In addition we restrict our attention to perturbations satisfying a zero-mass assumption (no addition or loss of material), and therefore the applicable values of k are $k=2n\pi$, where $n\in\mathbb{N}$. Moreover, it is possible to choose the rescaling in order that the perturbation represented by any relevant wave number $k=2n\pi$, where $n\geq 2$, can be scaled to represent the cosine function over a single wavelength (where $k=2\pi$) on the chosen domain (recall the non-dimensionalisation in section 3). Thus the only relevant wave number is $k=2\pi$.

6. The role of cell death on pattern formation

Having found expressions for planar and non-planar biofilm growth, focus is turned to determining the effect of different death terms on the growth of the biofilm. The role of cell death in the evolution of patterns is of particular interest and is now investigated.

It can be seen from equation (5.10) that in the absence of cell death, the dispersion relation $\omega(k,t)$ reduces to

$$\begin{aligned} \omega_a = \bar{S}\Bigg(1 - \frac{k\tanh(kh_0)}{\sqrt{G}}B_1 - \frac{k\tanh(kh_0)\tanh(\sqrt{G}h_0)}{\sqrt{G}} \\ + \frac{\sqrt{k^2+G}}{\sqrt{G}}\tanh(\sqrt{k^2+G}h_0)B_1\Bigg). \end{aligned} \tag{6.1}$$

In the presence of constant and substrate dependent cell death, the respective expressions for the dispersion relations at a specific h_0 are given by $\omega_c = (kh_0\tanh(kh_0)-1)\mu+\omega_a$ and $\omega_s = (kh_0\tanh(kh_0) - 1+\omega_a)\mu+\omega_a$.

At first glance it appears that the term $(kh_0\tanh(kh_0)-1)\mu$ in ω_c represents the effect of the bacterial death in the constant cell death case, suggesting that for kh_0 small enough, the introduction of $\mu>0$ contributes an extra negative term in ω_c, which switches to an extra positive term as h_0 increases. Therefore the model seems to predict that at the early stage of biofilm growth (where h_0 is small), a constant rate of bacterial death will stabilise planar growth to heterogeneous perturbations while at the

mature stage of biofilm growth (where h_0 is large), constant bacterial death will destabilise the planar height growth. These observations suggest constant bacterial death facilitates spatial pattern formation in mature biofilms. However, recalling that $h_0 = h_0(\mu)$, it is clear that ω_a is also dependent on μ, and thus the effect of cell death is not incorporated solely within the expression $(kh_0 \tanh(kh_0) - 1)\mu$, but rather within all terms in ω_c. Similar arguments follow for substrate dependent cell death: cell death is present in all terms in ω_s. As a result, a comparison of the planar solutions and behaviour of the dispersion relations ω_c and ω_s with respect to cell death is not as straightforward as appears at first sight. In order to investigate the behaviour of non-planar growth further, we now carry out a closer inspection at some extreme values in order to quantify certain qualitative features.

The first case considered assumes biofilm height at steady state is much less than the depth of the active layer, l_s, and thus substrate concentration is plentiful (a characteristic of early biofilms [31]) and approaching S_∞ throughout the entire biofilm depth. Recalling that $G = w^2/l_s^2$, it is clear that in the non-dimensional setting, the approximation $h_0^* \ll 1/\sqrt{G}$ can be used to represent this situation, and thus we refer to the biofilm as being 'shallow'. In this case the substrate dependent death term $d(S) \approx \mu(1 - S_\infty)$, and therefore cell death remains approximately constant at its minimum rate everywhere in the biofilm. Using $h_0^* \ll 1/\sqrt{G}$, the substitution of $\tanh(\sqrt{G}h_0^*) \simeq \sqrt{G}h_0^*$ can be made in equation (4.10) in order to find the non-trivial steady states h_{0c}^* and h_{0s}^* of shallow biofilms. The steady states are given by

$$h_{0c}^* = \frac{K(1-\mu)}{\mu GL}, \quad h_{0s}^* = \frac{K}{\mu GL}. \tag{6.2}$$

Note that in order to satisfy the shallow biofilm assumption, the value of the death parameters μ_c (in the case of constant cell death) and μ_s (in the case of substrate dependent cell death) must be sufficiently high, specifically

$$\mu_c \gg \frac{K}{K + L\sqrt{G}}, \quad \mu_s \gg \frac{K}{L\sqrt{G}}. \tag{6.3}$$

Using equation (6.2), the dependence of ω^* on μ can be explicitly defined in the case of shallow biofilms. Substitution of either h_{0c}^* or h_{0s}^* from equation (6.2) into ω^* (equation (5.11)) yields

$$\begin{aligned} \omega^* = &- B_{1S}^* \frac{\mu}{\sqrt{G}} \left(k \tanh(kh_0^*) - \sqrt{k^2 + G} \tanh(\sqrt{k^2 + G}h_0^*) \right) \\ &< 0, \end{aligned} \tag{6.4}$$

where

$$B_{1S}^* = -\sqrt{G} \left(\frac{k(K-1)h_0^* + \tanh(kL)}{Kk + \sqrt{k^2 + G} \tanh(\sqrt{k^2 + G}h_0^*) \tanh(kL)} \right) < 0. \tag{6.5}$$

As $\omega^* < 0$ for all wave numbers, it is clear that perturbations will not grow in shallow biofilms in either case of cell death. Therefore, in the long term, it is predicted that shallow biofilms will display no pattern formation.

In comparison to 'shallow' biofilms, we refer to 'deep' biofilms in the instances where the depth of the biofilm far exceeds the depth of the active layer, and represent this by assuming $h_0^* \gg 1/\sqrt{G}$. In this case, a large part of the biofilm is subjected to substrate deprivation, with the bottom region being the most adversely affected. This is indicative of mature biofilms [31]. A consequence of the assumption $h_0^* \gg 1/\sqrt{G}$ is that the approximation $\tanh(\sqrt{G}h_0^*) \simeq 1$ can be made. The non-trivial steady states for deep biofilms in the presence of cell death are found from equation (4.10) and are given by

$$h_{0c}^* = \frac{K}{\mu\sqrt{G}(K + L\sqrt{G})}, \quad h_{0s}^* = \left(1 + \frac{1}{\mu}\right) \frac{K}{\sqrt{G}(K + L\sqrt{G})}, \tag{6.6}$$

which are again explicitly dependent on μ, where μ must be sufficiently small, specifically

$$\mu_c \ll \frac{K}{K + L\sqrt{G}}, \quad \mu_s \ll \frac{K}{L\sqrt{G}}, \tag{6.7}$$

to be consistent with the condition $h_0^* \gg 1/\sqrt{G}$. In this case,

$$\begin{aligned} \omega_c^* =& \eta_c^* - \mu, \\ \omega_s^* =& \eta_s^*(1+\mu) - \mu, \end{aligned} \tag{6.8}$$

for $\eta_c^* = \eta(h_{0c}^*)$ and $\eta_s^* = \eta(h_{0s}^*)$, where

$$\eta(h) = \frac{K}{K + L\sqrt{G}} \left(1 - \frac{B_{1L}}{\sqrt{G}} \left(k \tanh(kh) - \sqrt{k^2 + G}\right)\right), \tag{6.9}$$

and

$$B_{1L} = -\frac{k(K-1) + \sqrt{G}\tanh(kL)}{Kk + \sqrt{k^2+G}\tanh(kL)} < 0. \tag{6.10}$$

(Note that B_{1L} is independent of μ, h_0 and h_0^*, and that $|B_{1L}| < 1$.)

As noted previously, it is clear that an increase in μ decreases the steady states h_{0c}^* and h_{0s}^*, which in turn lowers η^* (see equations (6.6) and (6.9)). It is therefore apparent from equation (6.8) that $\partial\omega_c^*/\partial\mu < 0$, and thus increased (constant) cell death has a stabilising effect on non-planar perturbations to h_{0c}^*. Since $\eta < 1$, it can also be shown that $\partial\omega_s^*/\partial\mu < 0$, and therefore it can be stated that, overall, an increase in μ has a stabilising effect on non-planar perturbations to h_{0s}^*.

Recalling Section 5.2, it is clear that in order to investigate the possibility of pattern formation occuring in deep biofilms satisfying the specified boundary conditions, behaviour of the dispersion relations ω_c^* and ω_s^* must be analysed at the relevant wave number, $k = 2\pi$. Therefore, substitution of $k = 2\pi$ and h_{0c}^* and h_{0s}^* from equation (6.6) into equations (6.8)-(6.10) give the values of $\eta(h)$, B_{1L} and subsequently ω^* that must be considered:

$$\eta(h_{0c}^*, k = 2\pi) = \frac{K}{K + L\sqrt{G}} \left(1 - \frac{B_{1L}}{\sqrt{G}} \left(2\pi \tanh\left(\frac{2\pi K}{\mu\sqrt{G}(K + L\sqrt{G})}\right) - \sqrt{4\pi^2 + G}\right)\right), \tag{6.11a}$$

$$\eta(h_{0s}^*, k = 2\pi) = \frac{K}{K + L\sqrt{G}} \left(1 - \frac{B_{1L}}{\sqrt{G}} \left(2\pi \tanh\left(\frac{2\pi K(1+\mu)}{\mu\sqrt{G}(K + L\sqrt{G})}\right) - \sqrt{4\pi^2 + G}\right)\right), \tag{6.11b}$$

where

$$B_{1L}(k = 2\pi) = -\frac{2\pi(K-1) + \sqrt{G}\tanh(2\pi L)}{2\pi K + \sqrt{4\pi^2+G}\tanh(2\pi L)} < 0. \tag{6.12}$$

As both $\partial\omega_c^*/\partial\mu < 0$ and $\partial\omega_s^*/\partial\mu < 0$ for any fixed k and any h_0^*, it follows that in the case of deep biofilms, the maximum values of $\omega_c^*(k = 2\pi)$ and $\omega_s^*(k = 2\pi)$ can be found by taking the limits as $\mu \to 0$. We find that

$$\begin{aligned} \lim_{\mu\to 0} \omega_c^*(k = 2\pi) &= \lim_{\mu\to 0} \eta(h_{0c}^*, k = 2\pi) \\ &= \frac{K}{K + L\sqrt{G}} \left(1 - \frac{B_{1L}(k = 2\pi)}{\sqrt{G}} \left(2\pi - \sqrt{4\pi^2 + G}\right)\right) \\ &\geq \frac{K}{K + L\sqrt{G}} \left(1 + B_{1L}(k = 2\pi)\right) \\ &> 0. \end{aligned} \tag{6.13}$$

Similarly, it can be shown that

$$\lim_{\mu\to 0} \omega_s^*(k = 2\pi) > 0. \tag{6.14}$$

Thus, in both regimes of cell death, the wave number $k = 2\pi$ is unstable to perturbations for sufficiently small μ.

In the case of constant cell death, the condition $\partial\omega_c^*/\partial\mu < 0$ holds. Also, as $\lim_{\mu\to 0} \omega_c^*(k = 2\pi) > 0$, it follows that as μ transits some critical value μ_c^{crit}, the stability of the wave number $k = 2\pi$ changes. This critical value is defined implicitly by the equation

$$\omega_c^*(\mu_c^{crit}, k = 2\pi) = \eta(h_{0c}^*(\mu_c^{crit}), k = 2\pi) - \mu_c^{crit} = 0. \tag{6.15}$$

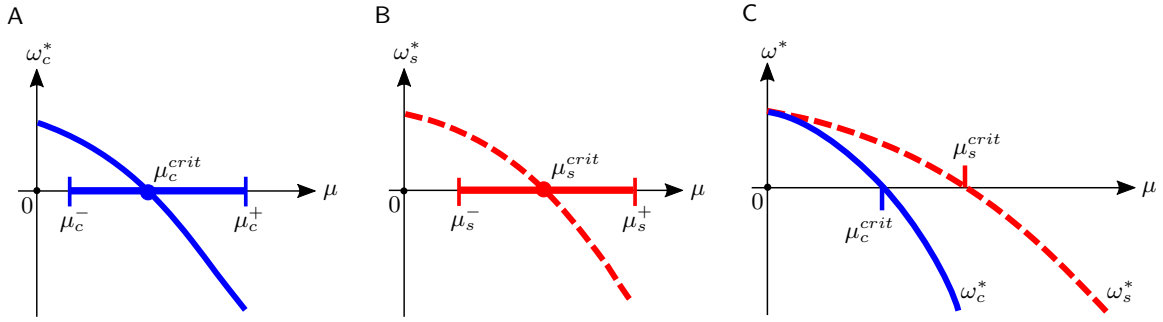

FIGURE 3. Schematic representation of dispersion relations $\omega^*(k = 2\pi)$ as functions of μ, in the case of $\sqrt{G}h_0^* \gg 1$. Figure A: Plot showing ω_c^*, which passes through μ_c^{crit}, where $\mu_c^- < \mu_c^{crit} < \mu_c^+$. Figure B: Plot showing ω_s^*, which passes through μ_s^{crit}, where $\mu_s^- < \mu_s^{crit} < \mu_s^+$. Figure C: Schematic showing both ω_c^* (blue solid line) and ω_s^* (red dashed line), where the relative positions of μ_c^{crit} and μ_s^{crit} are labelled.

We have:

$$\omega_c^* > 0 \text{ (growing perturbations) for } k = 2\pi \text{ if } \mu < \mu_c^{crit}, \tag{6.16a}$$

$$\omega_c^* < 0 \text{ (decaying perturbations) for } k = 2\pi \text{ if } \mu > \mu_c^{crit}, \tag{6.16b}$$

(see Figure 3A). It is possible to find an interval in which the implicitly defined value μ_c^{crit} lies by considering other aspects of the problem as follows. It can be shown that $\partial\omega_c^*/\partial k > 0$, and as such the limits as $k \to 0$ and $k \to \infty$ give the threshold values of μ, denoted μ_c^- and μ_c^+, for which all wave numbers $k > 0$ in ω_c^* can be said to be unstable or stable, respectively. We have $\omega_c^* > 0$ for all $k > 0$ if $\mu < \mu_c^-$ and $\omega_c^* < 0$ for all $k > 0$ if $\mu > \mu_c^+$, where

$$\mu_c^- = \frac{K}{(K + L\sqrt{G})^2}, \quad \mu_c^+ = \frac{K}{K + L\sqrt{G}}. \tag{6.17}$$

Thus it is clear that μ_c^{crit} must lie in the interval defined by

$$\mu_c^- < \mu_c^{crit} < \mu_c^+, \tag{6.18}$$

(again see Figure 3A). Recalling condition (6.7), it can be seen that for any value of $\mu > \mu_c^+$, the assumption of deep biofilms ($h_{0c}^* \gg 1/\sqrt{G}$) does not hold. Therefore any $\mu > \mu_c^+$ is irrelevant in our analysis of deep biofilms subject to constant cell death.

In the case of substrate dependent cell death, the conditions $\partial\omega_s^*/\partial\mu < 0$ and $\lim_{\mu\to 0}\omega_s^*(k = 2\pi) > 0$ hold. As above, it follows that as μ transits some critical value, denoted μ_s^{crit}, the sign of ω_s^* changes. Again we note that while μ_s^{crit} cannot be defined explicitly, it is implicitly defined by

$$\omega_s^*(\mu_s^{crit}, k = 2\pi) = \eta(h_{0s}^*(\mu_s^{crit}), k = 2\pi) \cdot (1 + \mu_s^{crit}) - \mu_s^{crit} = 0, \tag{6.19}$$

and the following conditions hold:

$$\omega_s^* > 0 \text{ (growing perturbations) for } k = 2\pi \text{ for } \mu < \mu_s^{crit}, \tag{6.20a}$$

$$\omega_s^* < 0 \text{ (decaying perturbations) for } k = 2\pi \text{ for } \mu > \mu_s^{crit}. \tag{6.20b}$$

Using a similar method as described above, we use the fact that $\partial\omega_s^*/\partial k > 0$, and take the limits of ω_s^* as $k \to 0$ and $k \to \infty$, to define the threshold values of μ, denoted μ_s^- and μ_s^+, for which all wave numbers

$k > 0$ can be said to be unstable or stable, respectively. We have $\omega_s^* > 0$ for all $k > 0$ if $\mu < \mu_s^-$ and $\omega_s^* < 0$ for all $k > 0$ if $\mu > \mu_s^+$, where

$$\mu_s^- = \frac{K}{(K + L\sqrt{G})^2 - K}, \quad \mu_s^+ = \frac{K}{L\sqrt{G}}. \tag{6.21}$$

Clearly μ_s^{crit} lies in the interval

$$\mu_s^- < \mu_s^{crit} < \mu_s^+, \tag{6.22}$$

(see Figure 3B). Once again it follows from condition (6.7), that the assumption $h_{0s}^* \gg 1/\sqrt{G}$ does not hold for $\mu > \mu_s^+$ and thus for these values of μ, further analysis is irrelevant. Comparing the cases of constant and substrate dependent cell death it is clear that, for each fixed $k > 0$ and for a fixed set of parameter values, $\omega_c^* < \omega_s^*$. As a result, $\mu_c^{crit} < \mu_s^{crit}$ (see Figure 3C). Thus it is possible that, for a fixed set of parameter values, a single value of μ satisfying both $h_{0c}^* \gg 1/\sqrt{G}$ and $h_{0s}^* \gg 1/\sqrt{G}$ may be chosen such that the condition

$$\mu_c^{crit} < \mu < \mu_s^{crit} \tag{6.23}$$

holds. In this special case, it is clear that $\omega_c^*(k = 2\pi) < 0$ and $\omega_s^*(k = 2\pi) > 0$. Thus, the wave number $k = 2\pi$ is unstable to perturbations in the case of substrate dependent cell death but is stable in the case of constant cell death. As a result, it is predicted that for values of μ in the interval defined by condition (6.23), patterning may occur in the case of substrate dependent cell death but will not occur in the case of constant cell death.

7. Conclusions

In this paper we introduced an extension of the model of Dockery and Klapper [13] to investigate the role of cell death in biofilm growth and wrinkle formation. It was found that the existence of a non-trivial steady state in the presence of both constant and substrate dependent cell death limits biofilm growth. While a sufficiently high death rate, μ, was found to induce complete biofilm die-back in the case of constant cell death, complete biofilm collapse was precluded, independent of the size of μ, in the case of substrate dependent cell death. In the cases where complete die-back did not occur, it was found that cell death played a key role in determining steady state biofilm height. As one might anticipate, the steady state biofilm height was predicted to decrease with increasing cell death rate.

In addition to determining the effect of cell death on biofilm height, our analysis also revealed the role of cell death in pattern formation. By analysing the evolution of non-planar perturbations to the non-trivial steady state, it was found that there is potential for spatial patterns to arise in deep biofilms. Moreover, the possibility of patterns evolving in shallow (early-stage) biofilms was ruled out. Experimental results have shown that during development, wildtype *B. subtilis* biofilms initially grow in height until reaching a critical thickness at which point vertical growth slows in lieu of horizontal expansion [29, 37]. It is also commonly observed that patterning occurs in mature (deep) biofilms [1, 5, 33]. Thus our analysis is in accordance with observed biological results.

Recent experimental observations by Asally et al. [1] showed that cell death focussed at the base of biofilms can induce patterning in biofilms. Interestingly, our analysis shows that biofilms subject to substrate dependent cell death at a certain rate μ could potentially exhibit pattern formation, whereas biofilms subject to constant cell death at the same rate are predicted to exhibit no pre-patterning behaviour. In summary, our analysis predicts that cell death focussed at the base of the biofilm is more likely to generate patterns, and is thus in line with the results of [1].

In conclusion, we propose that cell death may act as a precursor to patterning in biofilms by generating an instability within the biofilm. As in [1], we suggest that this patterning is likely to be further acted upon by other mechanisms at work in the biofilm in order to generate large-scale wrinkles. Biofilm models incorporating additional biological (in particular the role of EPS [18]) and mechanical processes e.g. [15, 33], may provide a complementary understanding of biofilm pattern formation.

Acknowledgements. This work was supported by The Northern Research Partnership (L. Li) and The Queen's Scholarship from the University of Dundee (H. A. Wallace). We thank Prof. Nicola Stanley-Wall (University of Dundee) for her assistance with the experiments conducted by L. Li.

References

[1] M. Asally, M. Kittisopikul, P. Rué, Y. Du, Z. Hu, T. Çağatay, A. B. Robinson, H. Lu, J. Garcia-Ojalvo, G. M. Süel, *Localized cell death focuses mechanical forces during 3D patterning in a biofilm*, Proceedings of the National Academy of Sciences, 109 (2012), pp. 18891–18896.

[2] B. P. Ayati, I. Klapper, *A multiscale model of biofilm as a senescence-structured fluid*, Multiscale Modeling & Simulation, 6 (2007), pp. 347–365.

[3] M. M. Baum, A. Kainović, T. O'Keeffe, R. Pandita, K. McDonald, S. Wu, P. Webster, *Characterization of structures in biofilms formed by a Pseudomonas fluorescens isolated from soil*, BMC Microbiology, 9 (2009), p. 103.

[4] S. S. Branda, Å. Vik, L. Friedman, R. Kolter, *Biofilms: the matrix revisited*, Trends in Microbiology, 13 (2005), pp. 20–26.

[5] L. S. Cairns, L. Hobley, N. R. Stanley-Wall, *Biofilm formation by Bacillus subtilis: new insights into regulatory strategies and assembly mechanisms*, Molecular Microbiology, 93 (2014), pp. 587–598.

[6] J. W. Costerton, Z. Lewandowski, D. E. Caldwell, D. R. Korber, H. M. Lappin-Scott, *Microbial biofilms*, Annual Review of Microbiology, 49 (1995), pp. 711–745.

[7] J. W. Costerton, P. S. Stewart, E. Greenberg, *Bacterial biofilms: a common cause of persistent infections*, Science, 284 (1999), pp. 1318–1322.

[8] J. Crank, *Free and Moving Boundary Problems*, Clarendon Press Oxford, 1984.

[9] E. L. Cussler, *Diffusion: mass transfer in fluid systems*, Cambridge University Press, 2009.

[10] B. D'Acunto, L. Frunzo, M. Mattei, *Qualitative analysis of the moving boundary problem for a biofilm reactor model*, Journal of Mathematical Analysis and Applications, 438 (2016), pp. 474–491.

[11] E. K. Davenport, D. R. Call, H. Beyenal, *Differential protection from tobramycin by extracellular polymeric substances from Acinetobacter baumannii and Staphylococcus aureus biofilms*, Antimicrobial Agents and Chemotherapy, 58 (2014), pp. 4755–4761.

[12] M. E. Davey, G. A. O'toole, *Microbial Biofilms: from ecology to molecular genetics*, Microbiology and Molecular Biology Reviews, 64 (2000), pp. 847–867.

[13] J. Dockery, I. Klapper, *Finger formation in biofilm layers*, SIAM J. Appl. Math, 62 (2001), pp. 853–869.

[14] R. M. Donlan, *Biofilms: microbial life on surfaces*, Emerging infectious Diseases, 8 (2002), pp. 881–890.

[15] D. Espeso, A. Carpio, B. Einarsson, *Differential growth of wrinkled biofilms*, Physical Review E, 91 (2015), p. 022710.

[16] A. S. Fleischer, *Thermal Energy Storage Using Phase Change Materials: Fundamentals and Applications*, Springer, 2015.

[17] M. R. Frederick, C. Kuttler, B. A. Hense, H. J. Eberl, *A mathematical model of quorum sensing regulated EPS production in biofilm communities*, Theoretical Biology and Medical Modelling, 8 (2011), pp. 1–29.

[18] J. Gerwig, T. B. Kiley, K. Gunka, N. Stanley-Wall, J. Stülke, *The protein tyrosine kinases EpsB and PtkA differentially affect biofilm formation in Bacillus subtilis*, Microbiology, 160 (2014), pp. 682–691.

[19] C. Giverso, M. Verani, P. Ciarletta, *Branching instability in expanding bacterial colonies*, Journal of The Royal Society Interface, 12 (2015), p. 20141290.

[20] A. E. Goodman, K. C. Marshall, *Genetic Responses of Bacteria at Surfaces*, in Microbial Biofilms, H. M. Lappin-Scott and J. W. Costerton, eds., Cambridge University Press, 1995, pp. 80–98. Cambridge Books Online.

[21] L. Hall-Stoodley, P. Stoodley, *Evolving concepts in biofilm infections*, Cellular Microbiology, 11 (2009), pp. 1034–1043.

[22] C. S. Laspidou, B. E. Rittmann, *Modeling the development of biofilm density including active bacteria, inert biomass, and extracellular polymeric substances*, Water Research, 38 (2004), pp. 3349–3361.

[23] Z. Lewandowski, *Biofilms: Recent Advances in their Study and Control*, Harwood Academic Publishers, 2000, pp. 1–17.

[24] B. Q. Li, *Discontinuous Finite Elements in Fluid Dynamics and Heat Transfer*, Springer Science & Business Media, 2005.

[25] D. López, H. Vlamakis, R. Kolter, *Biofilms*, Cold Spring Harbor perspectives in Biology, 2 (2010), p. a000398.

[26] M. Mimura, H. Sakaguchi, M. Matsushita, *Reaction–diffusion modelling of bacterial colony patterns*, Physica A: Statistical Mechanics and its Applications, 282 (2000), pp. 283–303.

[27] G. O'Toole, H. Kaplan, R. Kolter, *Biofilm formation as microbial development*, Annual Review of Microbiology, 54 (2000), pp. 49–79.

[28] D. Schultz, P. G. Wolynes, E. B. Jacob, J. N. Onuchic, *Deciding fate in adverse times: sporulation and competence in Bacillus subtilis*, Proceedings of the National Academy of Sciences, 106 (2009), pp. 21027–21034.

[29] A. Seminara, T. E. Angelini, J. N. Wilking, H. Vlamakis, S. Ebrahim, R. Kolter, D. A. Weitz, M. P. Brenner, *Osmotic spreading of Bacillus subtilis biofilms driven by an extracellular matrix*, Proceedings of the National Academy of Sciences, 109 (2012), pp. 1116–1121.

[30] P. S. Stewart, *Diffusion in Biofilms*, Journal of Bacteriology, 185 (2003), pp. 1485–1491.

[31] P. S. Stewart, M. J. Franklin, *Physiological heterogeneity in biofilms*, Nature Reviews Microbiology, 6 (2008), pp. 199–210.

[32] Y. Tang, A. J. Valocchi, *An improved cellular automaton method to model multispecies biofilms*, Water Research, 47 (2013), pp. 5729–5742.

[33] M. Trejo, C. Douarche, V. Bailleux, C. Poulard, S. Mariot, C. Regeard, E. Raspaud, *Elasticity and wrinkled morphology of Bacillus subtilis pellicles*, Proceedings of the National Academy of Sciences, 110 (2013), pp. 2011–2016.

[34] X. Wang, S. A. Koehler, J. N. Wilking, N. N. Sinha, M. T. Cabeen, S. Srinivasan, A. Seminara, S. Rubinstein, Q. Sun, M. P. Brenner, et al., *Probing phenotypic growth in expanding Bacillus subtilis biofilms*, Applied microbiology and biotechnology, 100 (2016), pp. 4607–4615.

[35] J. S. Webb, M. Givskov, S. Kjelleberg, *Bacterial biofilms: prokaryotic adventures in multicellularity*, Current opinion in microbiology, 6 (2003), pp. 578–585.

[36] J. S. Webb, L. S. Thompson, S. James, T. Charlton, T. Tolker-Nielsen, B. Koch, M. Givskov, S. Kjelleberg, *Cell death in Pseudomonas aeruginosa biofilm development*, Journal of Bacteriology, 185 (2003), pp. 4585–4592.

[37] W. Zhang, A. Seminara, M. Suaris, M. P. Brenner, D. A. Weitz, T. E. Angelini, *Nutrient depletion in Bacillus subtilis biofilms triggers matrix production*, New Journal of Physics, 16 (2014), p. 015028.